

Bose Condensation of Long-Living Direct Excitons in an Off-Resonant Cavity

N. S. Voronova,^{1,2,*} I. L. Kurbakov,³ and Yu. E. Lozovik^{3,4,†}

¹*National Research Nuclear University MEPhI (Moscow Engineering Physics Institute), 115409 Moscow, Russia*

²*Russian Quantum Center, 143025 Skolkovo, Moscow region, Russia*

³*Institute for Spectroscopy RAS, 142190 Troitsk, Moscow, Russia*

⁴*MIEM, National Research University Higher School of Economics, 101000 Moscow, Russia*



(Received 26 July 2018; published 4 December 2018)

We propose a way to increase the lifetime of two-dimensional *direct* excitons and show the possibility to observe their macroscopically coherent state at temperatures much higher than that of indirect exciton condensation. For a single GaAs quantum well embedded in photonic layered heterostructures with subwavelength period, we predict the exciton radiative decay to be strongly suppressed. Quantum hydrodynamics joined with the Bogoliubov approach are used to study the Berezinskii-Kosterlitz-Thouless crossover in a finite exciton system with intermediate densities. Below the estimated critical temperatures, drastic growth of the correlation length is shown to be accompanied by a manyfold increase of the photoluminescence intensity.

DOI: [10.1103/PhysRevLett.121.235702](https://doi.org/10.1103/PhysRevLett.121.235702)

Despite long-standing theoretical predictions [1–3], experimental observation of a macroscopically coherent state of excitons—bound pairs of electrons and holes in a semiconductor—for decades remained a challenging task and a subject of heated discussions [4–10]. Exciton Bose-Einstein condensation (BEC), once realized, could provide a plethora of beautiful observable phenomena with excitons, such as stimulated backscattering and multiphoton coherence [11], topological effects [12], supersolidity [13], ballistic transport [14], spin vortices [15], spin currents [2,16], etc. One of the major obstacles on the way to achieve the BEC of excitons, together with inhomogeneities and excess of free carriers [17], is the high exciton radiative recombination rate which hinders effective thermalization. Therefore, attempts to experimentally achieve excitonic BEC were mostly focused on electronically engineered systems utilizing indirect excitons (IX) [2] in coupled quantum wells (CQWs) under the influence of electric field [5–8,10], which allow lifetimes longer than the characteristic timescales of relaxation. Compared to IX, direct excitons have lifetimes too short for effective cooling, and they recombine before reaching the condensed state. However, as they are more tightly bound and allow much higher densities, direct excitons would offer notably higher critical temperatures of BEC.

While electronic engineering was the most fruitful approach so far elongating the exciton lifetime and leading to coherence, there is yet another way to control their radiative properties, which utilizes *photonic* engineering. As is well known from cavity quantum electrodynamics, if an excited light source is embedded into a photonic material environment, its recombination can be greatly enhanced [18] or inhibited [19]. It can be vastly employed

in devices whose performance is limited by spontaneous emission, such as low-threshold lasers, heterojunction transistors, single photon emitters, etc. For example, ways to experimentally control the spontaneous emission rate were demonstrated for quantum dots (QDs) in laterally structured microcavities [20], as well as quantum wells (QWs) and QDs in two-dimensional photonic crystals [21]. In this Letter, we show the possibility to suppress direct exciton recombination in a single QW by embedding it into an off-resonant cavity. Then, hydrodynamic quantum field theory [22–25] joined with the Bogoliubov description is employed to investigate the Berezinskii-Kosterlitz-Thouless (BKT) crossover in the exciton gas at elevated densities, with and without the inclusion of external magnetic field.

Considering a single GaAs QW embedded in a periodic photonic heterostructure, we seek the gap opening up in the electromagnetic density of states. We propose a short-period (subwavelength) metallic-dielectric structure, so that the exciton recombination frequency appears well inside this band gap. Using metal is essential to enhance the contrast between the refractive indices of layers and suppress coupling to the in-plane guided photon modes. We assume a spatially separated cw pump (see, e.g., Ref. [26]) at a frequency ω_p outside the gap, which allows optically generated excitons to readily relax to lowest-energy states while moving to the central region of the sample [27]. To obtain the field distribution inside the medium and optimize the layer widths and their number, we numerically solve the Maxwell problem for electric field \mathbf{E} inside the structure.

In our work we consider two specific geometries. The first realization is based on an 8-nm GaAs QW embedded in

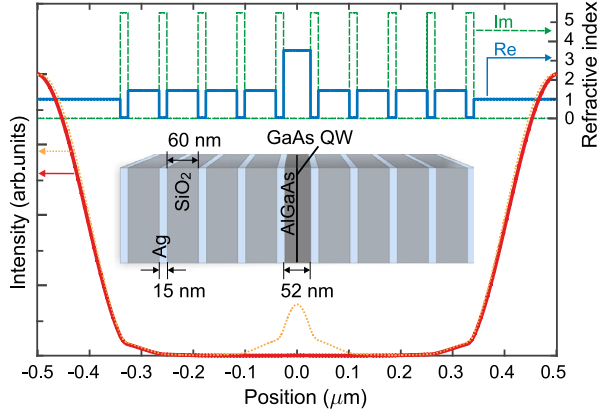


FIG. 1. Left axis: Intensity of field versus z (the layers growth direction), for the schematically illustrated layered structure. Red solid line: for $\omega_X = 1.57$ eV/ \hbar , suppression of light intensity in the QW region is $\sim 10^3$; orange dotted line: for pump frequency $\omega_P = 1.65$ eV/ \hbar . Right axis: Real (blue solid line) and imaginary (green dashed line) parts of the refractive index $\sqrt{\epsilon(z)}$ at the frequency ω_X .

a 52-nm AlGaAs (off-resonant) cavity layer sandwiched between the periodic structure with 4.5 pairs of Ag/SiO₂ layers (15/60 nm thickness, respectively), and is depicted schematically in Fig. 1. 8-nm QWs are well studied in works on IX, so we refer to the data of Ref. [29] with regard to direct exciton recombination line $\hbar\omega_X = 1.57$ eV and exciton lifetime without cavity $\tau_x = 70$ ps (recalculated for a single QW). Intensity distributions inside the structure are shown in Fig. 1, for the frequency corresponding to the exciton recombination and the pump frequency ($\hbar\omega_P = 1.65$ eV), first being suppressed by a factor of $\sim 10^3$, while the latter lies in the region of the cavity resonance [see also Fig. 2(a)] and has a maximum in the region of the QW [30].

Figure 2 summarizes the optical properties of the proposed structure. Radiative lifetimes for QW excitons inside the cavity were calculated as τ_x divided by $\langle |E|^2 \rangle$ in the region of the QW, for each in-plane wave vector k and frequency ω in consideration. Spectral dependence of the emission rate in the normal direction ($k = 0$) is shown in Fig. 2(a), whereas Fig. 2(b) provides inverse lifetimes of excitons with an in-plane wave vector k at the frequency ω_X . The obtained dependence $f(k) = 1/\tau(k)$ allows us to estimate the radiative lifetime of direct excitons in the system (see below), while for $k = 0$ one immediately deduces the lifetime in the ground state: $\tau(0) \approx 52$ ns. Figure 2(b) also shows that the parasitic optical recombination into the in-plane (guided) photon modes is suppressed [$f(k) \rightarrow 0$ as $ck/\omega \rightarrow 1$]. Figure 2(c) shows the dependence of the lifetime $\tau(0)$ on the number of layers in the structure. The complex dielectric constant of metallic layers results in dissipation of the field, for both ω_X and ω_P . Thus the optimal number of layers is chosen to provide lifetimes at ω_X long enough for thermalization (but not too

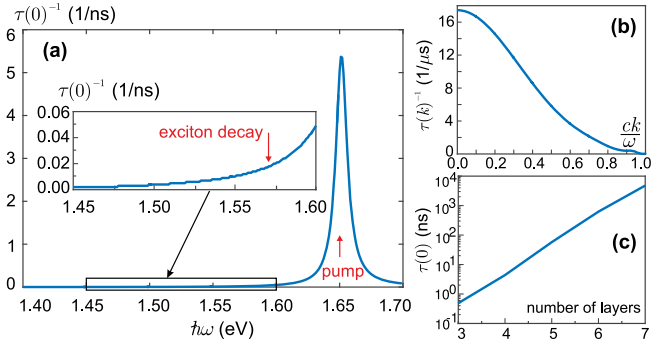


FIG. 2. Optical properties of the structure shown in Fig. 1. (a) Spectral dependence of inverse lifetime, deduced from the suppression of emission in the perpendicular direction. Red arrows mark the energies of the pump $\hbar\omega_P = 1.65$ eV and exciton optical recombination $\hbar\omega_X = 1.57$ eV (inset). For the latter, one deduces the lifetime $\tau(0) \approx 52$ ns. (b) Inverse lifetime of excitons with in-plane wave vector k at $\hbar\omega_X$, deduced from angular dependence of emission. (c) Lifetime of ground-state excitons versus number of layers.

long to avoid nonradiative recombination, which happens on microsecond timescales [31]), while keeping the line ω_P still enhanced [32].

The second geometry we suggest is based on the rapidly developing technology that allows selectively removing substrate and bonding thin layers (up to monolayers) of semiconductors. In order to elevate the exciton density and hence the BEC critical temperature, we consider an ultranarrow (2–4 monolayers) single GaAs QW embedded in a 40-nm AlGaAs layer sandwiched between 4.5 alternate layers of 20/30 nm thick Ag/SiO₂. In this ultranarrow case, fluctuations of the energy band gap due to fluctuations of Al and Ga concentrations in the AlGaAs barrier lead to a strong disorder. This can be overcome by, e.g., placing on both sides of the QW thin AlAs layers [33] or short-period superlattices $[(\text{GaAs})_x/(\text{AlAs})_y]_j$ ($x + y = 2, 3, 4$) representing a continuous medium for carriers [34]. For this geometry, the recombination energy is estimated as $\hbar\omega_X \approx 1.9$ eV and exciton lifetime without cavity $\tau_x \sim 10$ ps. The calculated lifetime of the ground-state excitons in this structure is $\tau(0) \approx 45$ ps. However, for such a thin QW the effect of dimensionality allows fourfold increase of the exciton density as compared to wider QWs [35], so the density can be taken as high as 3.2×10^{11} cm⁻², whereas for the 8-nm QW the lower estimate is $n = 8 \times 10^{10}$ cm⁻² [33].

The considered densities are much higher than IX densities in BEC experiments in CWQs [7,10]. At the same time, much smaller exciton Bohr radius ($a_B^X = 11$ nm for 8-nm QW and $a_B^X = 6$ nm for the ultranarrow QW) and higher binding energy of direct excitons prevents them from reaching Mott transition (which occurs in CQWs at $n = 2 \times 10^{10}$ cm⁻² and 12–16 K [36]). However, as we confirm below, the exciton gas at those densities is in the

regime of intermediate correlations and cannot be readily described by the mean field approximation. To achieve a better analytical description, we unify the Bogoliubov theory with the quantum hydrodynamic approach.

While in a macroscopic 2D uniform system BEC is forbidden [37], and only superfluid BKT transition takes place [38], in mesoscopic systems BEC can exist due to a slow decrease of the density matrix with temperature [23]. We will consider a finite but large 2D system of the size L , where the disappearance of BEC happens via the BKT crossover [39], and describe the behavior of the equilibrium one-body density matrix in the long-wavelength limit, i.e., at large $r \sim L$. The resulting expression has the form

$$\rho_1(\mathbf{r}) = n \exp \left[\frac{1}{S} \sum_{\mathbf{p} \neq 0} \frac{m \varepsilon_{\mathbf{p}} \kappa_{\mathbf{p}} e^{\varepsilon_{\mathbf{p}}/T} + 1}{2 \tilde{n}_s p^2 e^{\varepsilon_{\mathbf{p}}/T} - 1} \left(\cos \frac{\mathbf{p} \cdot \mathbf{r}}{\hbar} - 1 \right) \right] e^{-r/\xi_+}, \quad (1)$$

where m is the exciton mass, T is their temperature, $S = L^2$ is the quantization area, and \tilde{n}_s is the superfluid density renormalized by vortex pairs, as compared to the uniform superfluid density n_s [40]. An account of free vortices in the system is taken according to Kosterlitz [44] by introducing the factor e^{-r/ξ_+} (ξ_+ denotes the distance between free vortices [45]). The Bogoliubov spectrum of excitations $\varepsilon_{\mathbf{p}}$ is given by

$$\varepsilon_{\mathbf{p}} \equiv \sqrt{\frac{p^2}{m} \left(\frac{p^2}{4m} + U(\mathbf{p}) \tilde{n}_s \right)}, \quad (2)$$

where $U(\mathbf{p})$ contains contributions from two-, three-, and many-body interactions in the hydrodynamic Hamiltonian. The constant factor in Eq. (1) equals the total exciton density $n = \rho_1(0)$ and is defined consistently with the ultraviolet cutoff at short distances, $\kappa_{\mathbf{p}} = (1 - p^2/2m\varepsilon_{\mathbf{p}})^2$.

To estimate the effective interaction $U(\mathbf{p})$ in Eq. (2), one needs to consider a series of ladder diagrams which are dependent on the chemical potential μ due to the logarithmic divergence of the integrals at the lower limit in the case of small densities [46]. Following Mora and Castin [47], we expand the energy functional up to the third order in terms of a small density-dependent parameter $u(n)$, extrapolating the result of Ref. [47] to the crossover regime (i.e., intermediate correlations) comparing the analytically obtained expansion coefficients with the results of numerical simulations [48]. The bare interaction of direct excitons is described by the Lennard-Jones potential $U_{XX}(r) = W[(a^*/r)^{12} - (a^*/r)^6]$, with $a^* \sim a_B^X$. This interaction is short-ranged, so that $U(\mathbf{p})$ is weakly dependent on momenta. Hence we assume $U(\mathbf{p}) \approx U(0) = m^2 \chi^{-1}(0) = \partial^2 / \partial n^2 (E/S)$, $\chi(0)$ being the compressibility of the system. We obtain

$$U(\mathbf{p}) \approx \frac{2\pi \hbar^2 d^2(n^2 u)}{m \frac{dn^2}{dn^2}}, \quad (3)$$

where $u = u(n)$ is defined by the transcendental equation $1/u = C_3 u - \ln(\pi n a_s^2 u e^{2\gamma+1/2})$, $a_s > 0$ is the 2D wave-vector-dependent exciton scattering length [49], and $\gamma = 0.57721566\dots$ is Euler's constant. The numerical constant $C_3 \approx 2.298\dots$. Solving numerically the above equation for u with the parameters in consideration, one can estimate according to Eq. (3) the dimensionless adiabatic compressibility. For both structures, we get $m^3/4\pi \hbar^2 \chi(0) = \partial^2 / \partial n^2 (n^2 u/2) \approx 0.8$, which unambiguously indicates that correlations are not weak. Note that for a single-component uniform superfluid in the limit of weak correlations ($u \ll 1$) and low temperatures ($n - n_s \ll n_s$), expression (1) is accurate [48].

The superfluid density \tilde{n}_s in Eq. (1) is renormalized by the presence of vortex pairs with separations $\lesssim \min(r, \xi_+)$ and can be obtained from the problem of "dielectric" screening of the static supercurrent [38] as follows: $\tilde{n}_s = n_s^l / \varepsilon(x_+, a)$. Here $\varepsilon(x_+, a)$ is the effective scale-dependent "dielectric constant," $a \equiv 2\pi \hbar^2 n_s^l / mT$, n_s^l is the local superfluid density, and $x_+ \equiv \ln[\min(r, \xi_+)/l_0]$, l_0 being the healing length [50]. Then, for an infinite 2D system the BKT transition temperature is $T_c = \pi \hbar^2 n_s^l / 2m\varepsilon_\infty$ [51]. However, for a large finite system of the size L , the BKT crossover temperature is given by

$$T_c^L = \frac{\pi \hbar^2 n_s^l(T_c^L)}{2m\varepsilon_\infty} \left/ \left(1 - \frac{\pi^2 b^2}{[\ln(L/l_0) + \Delta]^2} \right) \right., \quad (4)$$

where the denominator is an analytical fit to the numerical calculation [52] with the parameters $\Delta \approx 2.93$, $b \approx 0.80$, and $\varepsilon_\infty \approx 1.135$. From Eq. (4), one obtains the distance between free vortices:

$$\xi_+ \sim \begin{cases} \infty & T < T_c \\ l_0 \exp(\pi b / \sqrt{1 - T_c/T} - \Delta) & T > T_c. \end{cases} \quad (5)$$

The local superfluid density n_s^l in Eqs. (4) and (5) is calculated with the use of the Landau formula,

$$n_s^l = n - \sum_{\sigma=1}^{\sigma_{\max}} \int \frac{d\mathbf{p}}{(2\pi \hbar)^2} \frac{p^2}{2mT} \frac{e^{\varepsilon_{\mathbf{p}\sigma}/T}}{(e^{\varepsilon_{\mathbf{p}\sigma}/T} - 1)^2}, \quad (6)$$

containing the spectrum of excitations $\varepsilon_{\mathbf{p}\sigma}$, where σ is the spin index and σ_{\max} is the spin degeneracy factor.

The results obtained above allow us to evaluate the asymptotic of the one-body density matrix Eq. (1), the true superfluid density n_s , and the condensate density n_0 as

$$n_s = \frac{n_s^l}{\varepsilon(\ln(L/l_0), a)}, \quad n_0 = \frac{1}{S} \int \rho_1(\mathbf{r}) d\mathbf{r}. \quad (7)$$

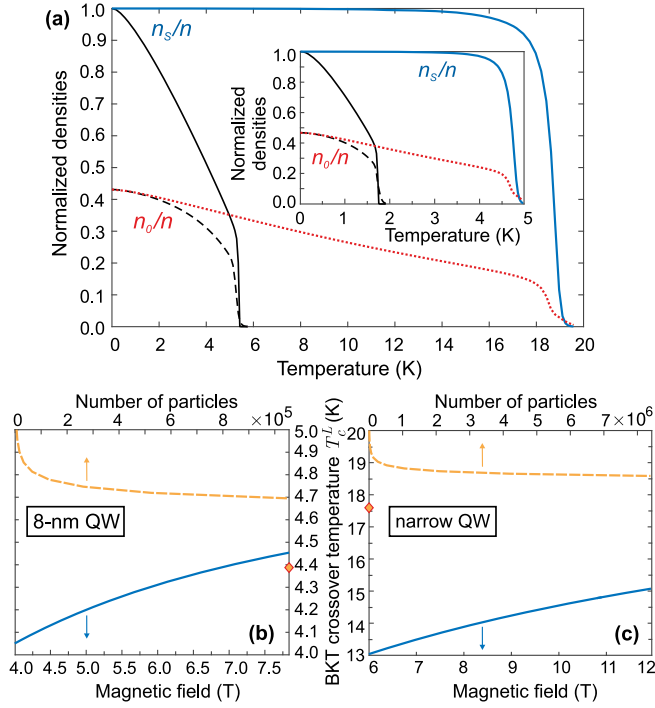


FIG. 3. (a) Normalized superfluid density n_s/n (blue solid line) and condensate density n_0/n (red dotted line) versus temperature for the ultranarrow QW, for the case when only one spin component is populated. The BKT crossover is clearly seen at $T_c^L \approx 19$ K. Physical parameters: total number of particles $N = 10^6$, $n = 3.2 \times 10^{11}$ cm $^{-2}$, $m = 0.22m_0$, $a_B^X = 6$ nm, $W = 10$ meV. Black solid and dashed lines show the same for a multicomponent system in the absence of the magnetic field [53]. Inset: Same for 8-nm QW, $T_c^L \approx 4.8$ K. Parameters are $N = 10^5$, $n = 8 \times 10^{10}$ cm $^{-2}$, $m = 0.22m_0$, $a_B^X = 11$ nm, $W = 3$ meV. (b), (c) Top axis, yellow dashed line: critical temperature T_c^L versus number of particles N (b) for 8-nm QW, at $n = 8 \times 10^{10}$ cm $^{-2}$ and (c) the ultranarrow QW, at $n = 3.2 \times 10^{11}$ cm $^{-2}$. Diamond marker on the vertical axis shows T_c^L for $N = \infty$. Bottom axis, blue solid line: T_c^L versus magnetic field H .

Figure 3(a) shows the results of calculations for the densities (7) depending on the temperature, revealing $T_c^L \approx 19$ K for the narrow QW realization and $T_c^L \approx 4.8$ K for the 8-nm GaAs QW. Dependence of the critical temperature Eq. (4) on the number of particles at a fixed density is shown in Figs. 3(b) and 3(c) for the 8-nm QW and the narrow QW, respectively.

So far, excitons were treated as spinless particles with the spectrum $\varepsilon_{p\sigma} \equiv \varepsilon_p$ given by Eq. (2). Taking into account four spin branches (in GaAs, $\sigma_{\max} = 4$) with exchange interactions [53] lowers T_c^L to 5 K (1.8 K) for the ultranarrow (8-nm) QW [shown as the black curves in Fig. 3(a)]. The spinless approximation, however, can be justified by employing the Zeeman effect. In order to analyze quantitatively at which magnetic fields one can neglect spin, we solve the BKT transition problem in magnetic field H to evaluate the spectrum $\varepsilon_{p\sigma}$ in the dilute and low-temperature

limit. In this case, the lowest branch is given by $\varepsilon_{p1} = \varepsilon_p$, while the higher branches have the form $\varepsilon_{p\sigma} = p^2/2m + D_\sigma$. Here $D_\sigma > 0$ are the Zeeman shifts in which all g factors are taken equal to 1, so that $D_\sigma/(e\hbar H/2mc) = 1, 3, 4$ at $\sigma = 2, 3, 4$. As one can see from Fig. 3(b), even for moderate fields the depletion of the superfluid component in the 8-nm QW is low: T_c^L is lowered less than by 15% (10%) at $H = 4$ T (6 T). This underlines the consistency of our spinless approximation. In the ultranarrow QW, the depletion of the superfluid component by the magnetic field is more pronounced [see Fig. 3(c)].

Finally, the exciton lifetime is defined by

$$\frac{1}{\tau} = \frac{1}{\tau(0)} \int \frac{d\mathbf{r}d\mathbf{k}}{(2\pi)^2 n} \rho_1(\mathbf{r}) e^{-r/\xi} \frac{f(k)}{f(0)} e^{i\mathbf{k}\cdot\mathbf{r}}, \quad (8)$$

where $f(k)$ is given in Fig. 2(b). The factor $e^{-r/\xi}$ indicates that the system is not fully thermalized at large scales: in thermal equilibrium, $\xi \rightarrow \infty$. According to Eq. (8), for the 8-nm (ultranarrow) QW we get $\tau \approx 150$ (140) ns. Keeping in mind that in CQWs, within the IX lifetimes $\tau_{IX} \sim 100$ ns [54], BEC occurs on the scales of the order of 12 μm [10], one concludes that for our structures, in the system of the size $L \sim \sqrt{N/n}$, the achieved lifetime is *a fortiori* long enough for thermalization.

It is important to note that finite lifetime does not affect the superfluidity in the system and the employed hydrodynamic formalism. Indeed, the time required for a wave packet to pass with the sound velocity $c_s = \sqrt{mn_s/\chi(0)}$ from one side of the system to the other, $t \sim L/c_s$, is 10^3 times shorter than τ . Hence, the sound damping is negligible, while the flow velocity produced by the exciton decay, $v \sim L/\tau$, is 10^3 times less than Landau critical velocity, $v_c \sim c_s$.

We complete our analysis by estimating the change in photoluminescence (PL) intensity in the region of the BKT crossover. During thermalization, τ drops after the appearance of the quasicondensate. In particular, as one can see in Fig. 4(a), in the absence of quasicondensate ($\xi_+ \sim 1/\sqrt{n}$), τ is approximately 2 orders of magnitude longer than when the coherence length is ~ 1 μm . The reason for this effect is the drastic narrowing of the k distribution of the system with the growth of the coherence length and appearance of quasicondensate, which pushes excitons into the cavity radiative region. As a result, excitons start to actively recombine, which can be seen in PL. Figure 4(b) displays sharp increase of the coherence length in the thermalized system at the crossover and the corresponding manifold growth of the emission intensity from the structure: as compared to intensity at $T > T_c^L$, it is 45 and 82 times higher below T_c^L for the 8-nm QW and the ultranarrow QW, respectively.

It should be mentioned that we assume QWs to be of a high quality with low inhomogeneities, e.g., the same as used in Ref. [10]. However, when disorder is taken into

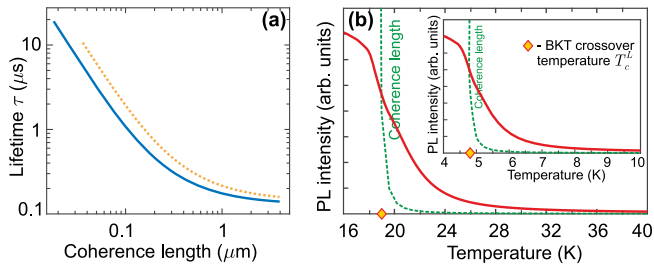


FIG. 4. (a) Lifetime of excitons with small momenta versus coherence length (blue solid line, for ultranarrow QW; yellow dotted line, for 8-nm QW). (b) Intensity of PL in direction close to normal (red solid line) versus temperature, for ultranarrow QW in thermal equilibrium. Green dashed line shows the coherence length versus T in arbitrary units, revealing its rise to infinity at T_c^L . Inset: Same for 8-nm QW. Parameters are the same as in Fig. 3.

account, critical temperatures are still estimated to be 4 K and higher [55].

In conclusion, we proposed a method to increase the lifetime of direct excitons in single GaAs QWs by employing photonic engineering, and predict their transition to the superfluid phase at temperatures from 4.8 to 19 K, depending on the geometry. For comparison, these values are well above $T_c = 0.1$ K demonstrated in CQWs [10], and are not lower than the temperatures theoretically estimated for IX superfluidity in spatially separated MoS_2 layers [56]. We would like to note that for excitons in a transition metal dichalcogenide (TMD) monolayer embedded in an off-resonant cavity, our theory predicts $T_c^L \approx 85$ K. However, the Auger processes being dominant in TMDs [57] present the main obstacle for exciton relaxation.

The authors are grateful to Oleg Kotov and Mikhail Glazov for discussions. N. S. V. acknowledges the financial support by the Russian Foundation for Basic Research, according to the research Project No. 16–32–60066 mol_a_dk, the Council of the President of the Russian Federation for Support of Young Scientists (Project No. MK–201.2017.2), and the Competitiveness Program of the NRNU MEPhI. Yu. E. L. is supported by the Program of Basic Research of the Higher School of Economics.

* nsvoronova@mephi.ru

† lozovik@isan.troitsk.ru

- [1] L. V. Keldysh and A. N. Kozlov, *Sov. Phys. JETP* **27**, 521 (1968).
- [2] Yu. E. Lozovik and V. I. Yudson, *Sov. Phys. JETP* **44**, 389 (1976).
- [3] X. Zhu, P. B. Littlewood, M. S. Hybertsen, and T. M. Rice, *Phys. Rev. Lett.* **74**, 1633 (1995).
- [4] J. L. Lin and J. P. Wolfe, *Phys. Rev. Lett.* **71**, 1222 (1993).
- [5] T. Fukuzawa, E. E. Mendez, and J. M. Hong, *Phys. Rev. Lett.* **64**, 3066 (1990).

- [6] L. V. Butov and A. I. Filin, *Phys. Rev. B* **58**, 1980 (1998).
- [7] L. V. Butov, C. W. Lai, A. L. Ivanov, A. C. Gossard, and D. S. Chemla, *Nature (London)* **417**, 47 (2002).
- [8] A. V. Larionov, V. B. Timofeev, P. A. Ni, S. V. Dubonos, I. Hvam, and K. Soerensen, *JETP Lett.* **75**, 570 (2002); V. B. Timofeev, *Phys. Usp.* **48**, 295 (2005).
- [9] A. V. Gorbunov and V. B. Timofeev, *JETP Lett.* **84**, 329 (2006); M. Alloing, M. Beian, M. Lewenstein, D. Fuster, Y. González, L. González, R. Combescot, M. Combescot, and F. Dubin, *Europhys. Lett.* **107**, 10012 (2014).
- [10] A. A. High, J. R. Leonard, A. T. Hammack, M. M. Fogler, L. V. Butov, A. V. Kavokin, K. L. Campman, and A. C. Gossard, *Nature (London)* **483**, 584 (2012).
- [11] Yu. E. Lozovik and I. V. Ovchinnikov, *JETP Lett.* **74**, 288 (2001); *Phys. Rev. B* **66**, 075124 (2002).
- [12] C.-E. Bardyn, T. Karzig, G. Refael, and T. C. H. Liew, *Phys. Rev. B* **91**, 161413(R) (2015).
- [13] I. L. Kurbakov, Yu. E. Lozovik, G. E. Astrakharchik, and J. Boronat, *Phys. Rev. B* **82**, 014508 (2010).
- [14] A. V. Kavokin, M. Vladimirova, B. Jouault, T. C. H. Liew, J. R. Leonard, and L. V. Butov, *Phys. Rev. B* **88**, 195309 (2013).
- [15] H. Sigurdsson, T. C. H. Liew, O. Kyriienko, and I. A. Shelykh, *Phys. Rev. B* **89**, 035302 (2014).
- [16] A. A. High, A. T. Hammack, J. R. Leonard, S. Yang, L. V. Butov, T. Ostatnický, M. Vladimirova, A. V. Kavokin, T. C. H. Liew, K. L. Campman, and A. C. Gossard, *Phys. Rev. Lett.* **110**, 246403 (2013).
- [17] V. V. Soloviev, I. V. Kukushkin, J. Smet, K. von Klitzing, and W. Dietsche, *JETP Lett.* **83**, 553 (2006).
- [18] E. M. Purcell, *Phys. Rev.* **69**, 681 (1946).
- [19] D. Kleppner, *Phys. Rev. Lett.* **47**, 233 (1981); E. Yablonovitch, *Phys. Rev. Lett.* **58**, 2059 (1987).
- [20] Y. Yamamoto, S. Machida, and G. Björk, *Phys. Rev. A* **44**, 657 (1991); M. Bayer, F. Weidner, A. Larionov, A. McDonald, A. Forchel, and T. L. Reinecke, *Phys. Rev. Lett.* **86**, 3168 (2001).
- [21] M. Fujita, S. Takahashi, Y. Tanaka, T. Asano, and S. Noda, *Science* **308**, 1296 (2005); A. Kress, F. Hofbauer, N. Reinelt, M. Kaniber, H. J. Krenner, R. Meyer, G. Böhm, and J. J. Finley, *Phys. Rev. B* **71**, 241304 (2005); D. Englund, D. Fattal, E. Waks, G. Solomon, B. Zhang, T. Nakaoka, Y. Arakawa, Y. Yamamoto, and J. Vučković, *Phys. Rev. Lett.* **95**, 013904 (2005).
- [22] V. N. Popov, *Functional Integrals in Quantum Field Theory and Statistical Physics* (Reidel, Dordrecht, 1983).
- [23] J. W. Kane and L. P. Kadanoff, *Phys. Rev.* **155**, 80 (1967).
- [24] P. Minnhagen and G. G. Warren, *Phys. Rev. B* **24**, 2526 (1981).
- [25] S. Giorgini, L. Pitaevskii, and S. Stringari, *Phys. Rev. B* **49**, 12938 (1994).
- [26] A. T. Hammack, M. Griswold, L. V. Butov, L. E. Smallwood, A. L. Ivanov, and A. C. Gossard, *Phys. Rev. Lett.* **96**, 227402 (2006).
- [27] See the Supplemental Material at <http://link.aps.org/supplemental/10.1103/PhysRevLett.121.235702> for discussion of the possibility to use electrical injection, which includes Ref. [28].
- [28] J. T. Leonard, E. C. Young, B. P. Yonkee, D. A. Cohen, T. Margalith, S. P. DenBaars, J. S. Speck, and S. Nakamura, *Appl. Phys. Lett.* **107**, 091105 (2015).

- [29] L. V. Butov, A. Imamoglu, A. V. Mintsev, K. L. Campman, and A. C. Gossard, *Phys. Rev. B* **59**, 1625 (1999).
- [30] See the Supplemental Material at <http://link.aps.org/supplemental/10.1103/PhysRevLett.121.235702> for the calculation details of the Maxwell problem.
- [31] V. V. Soloviev, I. V. Kukushkin, J. Smet, K. von Klitzing, and W. Dietsche, *JETP Lett.* **84**, 222 (2006).
- [32] See the Supplemental Material at <http://link.aps.org/supplemental/10.1103/PhysRevLett.121.235702> for the account of losses.
- [33] R. Eccleston, B. F. Feuerbacher, J. Kuhl, W. W. Rühle, and K. Ploog, *Phys. Rev. B* **45**, 11403 (1992).
- [34] S.-F. Ren, J.-B. Xia, H.-X. Han, and Z.-P. Wang, *Phys. Rev. B* **50**, 14416 (1994).
- [35] 2D exciton Bohr radius a_B^X is known to be 2 times smaller than in 3D, its binding energy E_b and $1/(a_B^X)^2$ are 4 times higher. Therefore, for an ultranarrow QW, densities can be assumed 4 times as high as in a very wide (27-nm) QW [33], where E_b and $1/(a_B^X)^2$ are almost the same as in bulk. See L. C. Andreani and A. Pasquarello, *Phys. Rev. B* **42**, 8928 (1990).
- [36] G. Kiršanskė, P. Tighineanu, R. S. Daveau, J. Miguel-Sánchez, P. Lodahl, and Soren Støbbe, *Phys. Rev. B* **94**, 155438 (2016).
- [37] P. C. Hohenberg, *Phys. Rev.* **158**, 383 (1967).
- [38] J. M. Kosterlitz and D. J. Thouless, *J. Phys. C* **6**, 1181 (1973).
- [39] Z. Hadzibabic, P. Krüger, M. Cheneau, B. Battelier, and J. Dalibard, *Nature (London)* **441**, 1118 (2006).
- [40] See Supplemental Material <http://link.aps.org/supplemental/10.1103/PhysRevLett.121.235702> for detailed derivation, which includes Refs. [41–43].
- [41] R. Kubo, *J. Phys. Soc. Jpn.* **17**, 1100 (1962).
- [42] P. Carruthers and M. M. Nieto, *Rev. Mod. Phys.* **40**, 411 (1968).
- [43] H.-F. Meng, *Phys. Rev. B* **49**, 1205 (1994).
- [44] J. M. Kosterlitz, *J. Phys. C* **7**, 1046 (1974).
- [45] V. Ambegaokar, B. I. Halperin, D. R. Nelson, and E. D. Siggia, *Phys. Rev. Lett.* **40**, 783 (1978).
- [46] Yu. E. Lozovik and V. I. Yudson, *Physica (Amsterdam)* **93A**, 493 (1978).
- [47] C. Mora and Y. Castin, *Phys. Rev. Lett.* **102**, 180404 (2009).
- [48] N. S. Voronova, I. L. Kurbakov, A. S. Pliashchnik, and Yu. E. Lozovik (to be published).
- [49] G. E. Astrakharchik, J. Boronat, I. L. Kurbakov, Yu. E. Lozovik, and F. Mazzanti, *Phys. Rev. A* **81**, 013612 (2010).
- [50] See the Supplemental Material at <http://link.aps.org/supplemental/10.1103/PhysRevLett.121.235702> for detailed derivation of the renormalized superfluid density \tilde{n}_s within the dielectric screening problem.
- [51] D. R. Nelson and J. M. Kosterlitz, *Phys. Rev. Lett.* **39**, 1201 (1977).
- [52] Yu. E. Lozovik, I. L. Kurbakov, and M. Willander, *Phys. Lett. A* **366**, 487 (2007).
- [53] For direct excitons, exchange energy is of the order of 0.01 meV [see H. Fu, L.-W. Wang, and A. Zunger, *Phys. Rev. B* **59**, 5568 (1999)], which corresponds to the magnetic field of the order of 0.1 T.
- [54] K. Sivalertporn, L. Mouchliadis, A. L. Ivanov, R. Philp, and E. A. Muljarov, *Phys. Rev. B* **85**, 045207 (2012).
- [55] See the Supplemental Material at <http://link.aps.org/supplemental/10.1103/PhysRevLett.121.235702> for the effects of disorder are investigated in Sec. IV.
- [56] M. M. Fogler, L. V. Butov, and K. S. Novoselov, *Nat. Commun.* **5**, 4555 (2014).
- [57] M. Kulig, J. Zipfel, P. Nagler, S. Blanter, C. Schüller, T. Korn, N. Paradiso, M. M. Glazov, and A. Chernikov, *Phys. Rev. Lett.* **120**, 207401 (2018).